

# Instability of holographic dark energy models

Yun Soo Myung\*

*Institute of Mathematical Science and School of Computer Aided Science  
Inje University, Gimhae 621-749, Korea*

## Abstract

We investigate the difference between holographic dark energy, Chaplygin gas, and tachyon model with constant potential. For this purpose, we examine their squared speeds of sound which are evaluated to zeroth order in perturbation theory and hence depends only on time. We find that the squared speed for holographic dark energy is always negative when choosing the future event horizon as the IR cutoff, while those for Chaplygin gas and tachyon are non-negative. This means that the perfect fluid for holographic dark energy is classically unstable. Hence the holographic interpretation for Chaplygin gas and tachyon is problematic.

---

\*e-mail address: ysmyoung@inje.ac.kr

# 1 Introduction

Observations of supernova type Ia suggest that our universe is accelerating [1]. Considering the  $\Lambda$ CDM model [2, 3], the dark energy and cold dark matter contribute  $\Omega_{\Lambda}^{\text{ob}} \simeq 0.74$  and  $\Omega_{\text{CDM}}^{\text{ob}} \simeq 0.22$  to the critical density of the present universe. Recently the combination of WMAP3 and Supernova Legacy Survey data shows a significant constraint on the equation of state (EOS) for the dark energy,  $w_{\text{ob}} = -0.97^{+0.07}_{-0.09}$  in a flat universe [4, 5].

Although there exist a number of dark energy models [6], the two promising candidates are the cosmological constant and the quintessence scenario [7]. The EOS for the latter is determined dynamically by the scalar or tachyon.

On the other hand, there exists another model of the dark energy arisen from the holographic principle. The authors in [8] showed that in quantum field theory, the ultra-violet (UV) cutoff  $\Lambda$  could be related to the infrared (IR) cutoff  $L$  due to the limit set by forming a black hole. If  $\rho_{\Lambda} = \Lambda^4$  is the vacuum energy density caused by the UV cutoff, the total energy for a system of size  $L$  should not exceed the mass of the system-size black hole:

$$E_{\Lambda} \leq E_{BH} \longrightarrow L^3 \rho_{\Lambda} \leq M_{\text{p}}^2 L. \quad (1)$$

If the largest cutoff  $L_{\Lambda}$  is chosen to be the one saturating this inequality, the holographic energy density is given by the energy density of a system-size black hole as

$$\rho_{\Lambda} = \frac{3c^2 M_{\text{p}}^2}{8\pi L_{\Lambda}^2} \quad (2)$$

with a constant  $c$ . Here we regard  $\rho_{\Lambda}$  as a dynamical cosmological constant. At the planck scale of  $L_{\Lambda} = M_{\text{p}}^{-1}$ , it is just the vacuum energy density  $\rho_{\text{v}} = M_{\text{p}}^2 \Lambda_{\text{eff}}/8\pi$  of the universe at  $\Lambda_{\text{eff}} \sim M_{\text{p}}^2$ :  $\rho_{\Lambda} \sim \rho_{\text{p}} \sim M_{\text{p}}^4$ . This implies that a very small system has an upper limit on the energy density as expected in quantum field theory. On the other hand, a larger system gets a smaller energy density. If the IR cutoff is taken as the size of the current universe ( $L_{\Lambda} = H_0^{-1}$ ), the resulting energy density is close to the current dark energy:  $\rho_{\Lambda} \sim \rho_{\text{c}} \sim 10^{-123} M_{\text{p}}^4$  [9]. This results from the holography: the energy increases with the linear size, so that the energy density decreases with the inverse-area law. The total energy density dilutes as  $L_{\Lambda}^{-3}$  due to the evolution of the universe, whereas its upper limit set by gravity (black hole) decreases as  $L_{\Lambda}^{-2}$ .

It is not easy to determine the EOS for a system including gravity with the UV and IR cutoffs. If one considers  $L = H_0^{-1}$  together with the cold dark matter, the EOS may take the form of  $w_{\Lambda} = 0$  [10], which is just that of the cold dark matter. However, introducing an interaction between holographic dark energy and cold dark matter may

lead to an accelerating universe [11]. Interestingly, the future event (particle) horizons<sup>1</sup> were introduced to obtain the equations of state [12, 13, 14, 15, 16].

Recently, there was an attempt to make a correspondence between the holographic dark energy and Chaplygin gas [17]. Also the connection between the holographic dark energy and tachyon model [18, 19, 20] was introduced to explain the dark energy [21, 22]. In the cases of Chaplygin gas with  $p = -A/\rho$  [23, 24] and tachyon model with  $V(T) = \sqrt{A}$  [25], one has the EOS range of  $-1 \leq \omega_{C,T} \leq 0$ . Also we have a similar range  $-1 \leq \omega_\Lambda \leq -1/3$  for the holographic dark energy with the future event horizon [12]. In spite of the similarity between the holographic dark energy model and Chaplygin gas (tachyon model), there exist differences. We consider the linear perturbation of holographic dark energy towards a dark energy-dominated universe. For this purpose, a key quantity is the squared speed of sound  $v^2 = dp/d\rho$  [26]. The sign of  $v^2$  is crucial for determining the stability of a background evolution. If this is negative, it means a classical instability of a given perturbation. It is known that the Chaplygin gas (tachyon) have the positive squared speeds of sound with  $v_{C,T}^2 = -\omega_{C,T}$  and thus they are supposed to be stable against small perturbations [27, 28]. Interestingly, the squared speed of sound takes a similar form like the statefinder parameters  $\{r, s\}$  [29], which can probe the dynamical evolution of the universe through the higher derivatives  $d^3a/dt^3$  of the scale factor  $a$  [30, 31].

In this Letter, we address this issue for the holographic dark energy model. We compare the holographic dark energy model with the Chaplygin gas and tachyon model to show its unstable evolution.

## 2 Squared speed for holographic dark energy

In this section we discuss the flat universe. If the holographic dark energy density  $\rho_\Lambda = \frac{3c^2 M_p^2}{8\pi L_\Lambda^2}$  is known with the IR cutoff  $L_\Lambda$ , its pressure is determined solely by the conservation of energy-momentum tensor with  $x = \ln a$  [13]

$$p_\Lambda = -\frac{1}{3} \frac{d\rho_\Lambda}{dx} - \rho_\Lambda \quad (3)$$

which provides the EOS

$$\omega_\Lambda = \frac{p_\Lambda}{\rho_\Lambda} = -1 + \frac{2}{3H} \frac{\dot{L}_\Lambda}{L_\Lambda}. \quad (4)$$

Hence, if one does not choose an appropriate form of  $L_\Lambda$ , one cannot find its EOS. For example, if one chooses the Hubble horizon  $L_\Lambda = 1/H_0$ , it does not provide the

---

<sup>1</sup>Here, we introduce the definition of the future event horizon  $R_{\text{FH}} = a(t) \int_t^\infty \frac{dt'}{a(t')}$  and the particle horizon  $R_{\text{PH}} = a(t) \int_0^t \frac{dt'}{a(t')}$  with the flat Friedmann-Robertson-Walker metric  $ds_{\text{FRW}}^2 = -dt^2 + a^2(t)d\mathbf{x} \cdot d\mathbf{x}$ .

correct EOS [10]. Here we have  $\dot{H} = -\frac{3}{2}H^2(1 + \omega_\Lambda)$ , which is nothing but the second Friedmann equation. On the other hand, choosing  $L_\Lambda = R_{\text{PH/FH}} = c/H\sqrt{\Omega_\Lambda}$  with  $\Omega_\Lambda = 8\pi\rho_\Lambda/3M_p^2H^2$  leads to

$$\omega_\Lambda^{\text{PH/FH}} = -\frac{1}{3}\left(1 \mp \frac{2}{c}\sqrt{\Omega_\Lambda}\right) \quad (5)$$

because the definition of the holographic dark energy density implies

$$\dot{\rho}_\Lambda = 2H\rho_\Lambda\left[-1 \mp \frac{1}{HR_{\text{PH/FH}}}\right] = -3H\rho_\Lambda\left[1 - \frac{1}{3} \pm \frac{2\sqrt{\Omega_\Lambda}}{3c}\right]. \quad (6)$$

$\omega_\Lambda$  is determined by the evolution equation

$$\frac{d\Omega_\Lambda}{dx} = \frac{\dot{\Omega}_\Lambda}{H} = -3\omega_\Lambda\Omega_\Lambda(1 - \Omega_\Lambda). \quad (7)$$

For our purpose, we introduce the squared speed of holographic dark energy fluid as

$$v_\Lambda^2 = \frac{dp_\Lambda}{d\rho_\Lambda} = \frac{\dot{p}_\Lambda}{\dot{\rho}_\Lambda}, \quad (8)$$

where

$$\dot{p}_\Lambda = \dot{\omega}_\Lambda\rho_\Lambda + \omega_\Lambda\dot{\rho}_\Lambda \quad (9)$$

with [30]

$$\dot{\omega}_\Lambda = H\frac{d\omega_\Lambda}{dx} = -\frac{H}{3c}\sqrt{\Omega_\Lambda}(1 - \Omega_\Lambda)\left(1 \mp \frac{2}{c}\sqrt{\Omega_\Lambda}\right). \quad (10)$$

It leads to

$$v_\Lambda^2 = \omega_\Lambda\left[1 - \frac{\sqrt{\Omega_\Lambda}(1 - \Omega_\Lambda)}{3c(1 + \omega_\Lambda)}\right] = \omega_\Lambda\left[1 - \frac{\sqrt{\Omega_\Lambda}(1 - \Omega_\Lambda)}{2(c \pm \sqrt{\Omega_\Lambda})}\right], \quad (11)$$

which contrasts to those for the Chaplygin gas and tachyon model

$$v_{\text{C,T}}^2 = -\omega_{\text{C,T}} \geq 0. \quad (12)$$

In the linear perturbation theory, the density perturbation is described by

$$\rho(t, \mathbf{x}) = \rho(t) + \delta\rho(t, \mathbf{x}) \quad (13)$$

with  $\rho(t)$  the background value. Then the conservation law for the energy-momentum tensor of  $\nabla_\nu T^{\mu\nu} = 0$  yields [32]

$$\delta\ddot{\rho} = v^2\nabla^2\delta\rho(t, \mathbf{x}), \quad (14)$$

where  $T^0{}_0 = -(\rho(t) + \delta\rho(t, \mathbf{x}))$  and  $v^2 = dp/d\rho$ . For  $v_{\text{C,T}}^2 > 0$ , Eq. (14) becomes a regular wave equation whose solution is given by  $\delta\rho_{\text{C,T}} = \delta\rho_{0\text{C,T}}e^{-i\omega t + i\mathbf{k}\cdot\mathbf{x}}$ . Hence the

Table 1: Summary for holographic dark energy (HDE), Chaplygin gas (CG), tachyon model (TM). For HDE, the conservation law determines its pressure because the energy density is known, while for CG, the conservation law determines the energy density because the pressure is known. Range of EOS for HDE is for the future event horizon.

	HDE	CG	TM
energy density	$\rho_\Lambda = 3c^2 M_p^2 / 8\pi L_\Lambda^2$	$\rho_C = \sqrt{A + B/a^6}$	$\rho_T = V/\sqrt{1 - \dot{T}^2}$
pressure	$p_\Lambda = \omega_\Lambda \rho_\Lambda$	$p_C = -A/\rho_C$	$p_T = -V\sqrt{1 - \dot{T}^2}$
EOS	$\omega_\Lambda = -1/3 \pm 2\sqrt{\Omega_\Lambda}/3c$	$\omega_C = -A/\rho_C^2$	$\omega_T = -1 + \dot{T}^2$
range of EOS	$-1 \leq \omega_\Lambda \leq -1/3$	$-1 \leq \omega_C \leq 0$	$-1 \leq \omega_T \leq 0$
squared speed	$v_\Lambda^2 = \omega_\Lambda \left[ 1 - \frac{\sqrt{\Omega_\Lambda}(1-\Omega_\Lambda)}{3c(1+\omega_\Lambda)} \right]$	$v_C^2 = A/\rho^2 = -\omega_C$	$v_T^2 = 1 - \dot{T}^2 = -\omega_T$

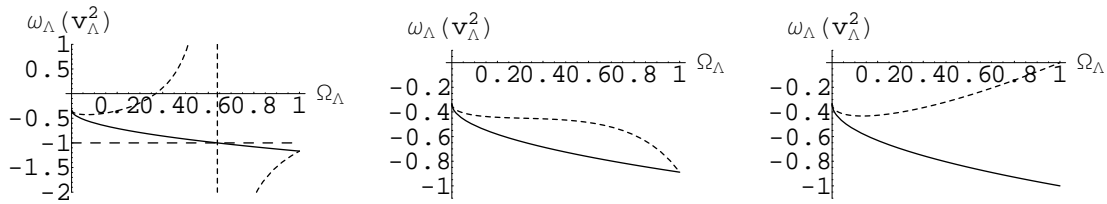


Figure 1: Three graphs for the holographic dark energy with the future event horizon. The solid (dashed) lines denote the equation of state  $\omega_\Lambda$  (squared speed  $v_\Lambda^2$ ). One has the graphs for  $c = 0.8$ ,  $c = 1$ , and  $c = 1.2$  from the left to the right.

positive squared speed (real value of speed) shows a regular propagating mode for a density perturbation. For  $v_\Lambda^2 < 0$ , the perturbation becomes an irregular wave equation whose solution is given by  $\delta\rho_\Lambda = \delta\rho_{0\Lambda}e^{\omega t + i\mathbf{k}\cdot\mathbf{x}}$ . Hence the negative squared speed (imaginary value of speed) shows an exponentially growing mode for a density perturbation. That is, an increasing density perturbation induces a lowering pressure, supporting the emergence of instability. In Table 1, we summarize the relevant quantities for holographic dark energy, Chaplygin gas, and tachyon model for comparison.

In the case of holographic dark energy with the future event horizon, one finds from Fig. 1 that the squared speed is always negative for the whole evolution  $0 \leq \Omega_\Lambda \leq 1$ . Especially, for  $c = 0.8 (< 1)$ , we have a discontinuity from  $v_\Lambda^2 = -\infty$  to  $\infty$  around  $\Omega_\Lambda = 0.64$  whose equation of state crosses  $\omega_\Lambda = -1$ . For example, we have  $v_\Lambda^2 = 229$  at  $\Omega_\Lambda = 0.639$  while we have  $v_\Lambda^2 = -231$  at  $\Omega_\Lambda = 0.641$ . This means that the phantom phase occurs when the squared speed of holographic dark energy blows up.

In the case of holographic dark energy with the particle horizon, one finds from Fig. 2 that the  $c = 1$  squared speed changes from  $-1/3$  to  $1/3$  as the universe evolves, which

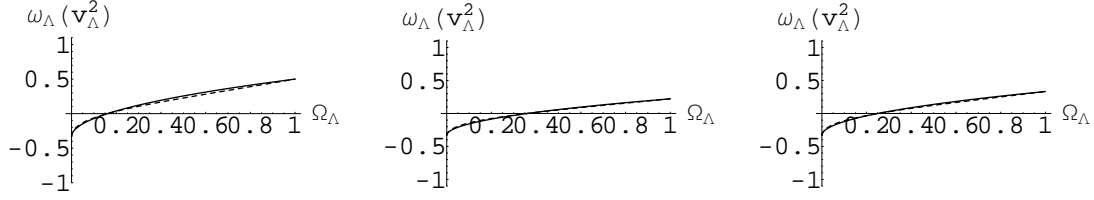


Figure 2: Three graphs for the holographic dark energy with the particle horizon. The solid (dashed) lines denote the equation of state  $\omega_\Lambda$  (squared speed  $v_\Lambda^2$ ). From the left to the right, one has the graphs for  $c = 0.8$ ,  $c = 1$ , and  $c = 1.2$ . There is no significant change between them.

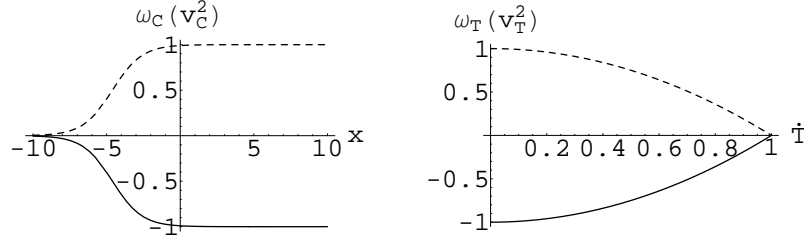


Figure 3: Two graphs for the Chaplygin gas and tachyon model. The left panel is for  $\omega_C(v_C^2)$  vs  $x = \ln a$ , while the right one is for  $\omega_T(v_T^2)$  vs  $\dot{T}$ . The solid (dashed) lines denote the equation of state  $\omega_{C,T}$ (squared speed  $v_{C,T}^2$ ). Here we find the positive squared speeds.

is nearly coherent with the equation of state. Also there is no sizable difference between  $c = 0.8, 1.0$  and  $1.2$  except slightly different loci for  $v_\Lambda^2 = 0$ . In this case, we read off the classical instability of  $v_\Lambda^2 < 0$  for  $-1/3 \leq \omega_\Lambda < 0$ . However, from Fig. 3 we have the non-negative squared speed in the Chaplygin gas model. This means that the Chaplygin gas is stable against the linear perturbation even though it could describe both the cold dark matter at the early universe and dark energy at the present and future universe. Also for the tachyon model with constant potential which is essentially the Chaplygin gas, we have the cold dark matter at  $\dot{T} = 1$  ( $T \rightarrow \infty, \ddot{T} = 0$ ) and dark energy at  $\dot{T} = 0$  ( $T \simeq \text{const}, \ddot{T} = 0$ ). On the other hand, for  $V(T) \simeq m^2(T - T_0)^2/2$ , fluctuations coupled to the oscillating background condensate were exponentially unstable and for pressureless tachyon with  $V(T) = V_0 e^{-T/T_0}$ , fluctuations coupled with metric perturbations also showed gravitational instability [25].

### 3 Squared speed for the nonflat universe

In this section, we attempt to find the squared speed for the nonflat universe. For this purpose, we introduce the density parameter for curvature defined by  $\Omega_k = \frac{k}{a^2 H^2}$ . Then we can rewrite the Friedmann equation as a simplified form

$$\Omega_\Lambda = 1 + \Omega_k. \quad (15)$$

For the non-flat universe of  $k \neq 0$ , we consider the future event horizon  $L_\Lambda = R_{\text{FH}} = a\xi_{\text{FH}}(t) = a\xi_{\text{FH}}^k(t)$  with

$$\xi_{\text{FH}}(t) = \int_t^\infty \frac{dt}{a}. \quad (16)$$

Here the comoving horizon size is given by

$$\xi_{\text{FH}}^k(t) = \int_0^{r(t)} \frac{dr}{\sqrt{1 - kr^2}} = \frac{1}{\sqrt{|k|}} \text{sinn}^{-1} \left[ \sqrt{|k|} r(t) \right], \quad (17)$$

which leads to  $\xi_{\text{FH}}^{k=1}(t) = \sin^{-1} r(t)$ ,  $\xi_{\text{FH}}^{k=0}(t) = r(t)$ , and  $\xi_{\text{FH}}^{k=-1}(t) = \sinh^{-1} r(t)$ . Here we introduce a comoving radial coordinate  $r(t)$ ,

$$r(t) = \frac{1}{\sqrt{|k|}} \text{sinn} \left[ \sqrt{|k|} \xi_{\text{FH}}^k(t) \right]. \quad (18)$$

Then  $L_\Lambda = ar(t)$  is a useful length scale for the non-flat universe [13]. Its derivative with respect to time  $t$  leads to

$$\dot{L}_\Lambda = HL_\Lambda + a\dot{r} = \frac{c}{\sqrt{\Omega_\Lambda}} - \text{cosny}, \quad (19)$$

where  $\text{cosny} = \text{cos} y$ ,  $y$ ,  $\text{cosh} y$  for  $k = 1, 0, -1$  with  $y = \sqrt{k} R_{\text{FH}}/a$ . One finds the equation of state for the holographic dark energy

$$\dot{\rho}_\Lambda + 3H \left[ 1 - \frac{1}{3} - \frac{2\sqrt{\Omega_\Lambda}}{3c} \text{cosny} \right] \rho_\Lambda = 0. \quad (20)$$

Here we can read off the EOS

$$\omega_\Lambda = -\frac{1}{3} - \frac{2\sqrt{\Omega_\Lambda - c^2\Omega_k}}{3c} = -\frac{1}{3} - \frac{2\sqrt{\Omega_\Lambda(1 - c^2) + c^2}}{3c}. \quad (21)$$

In this case, considering the evolution equation together with Eq.(15) leads to

$$\frac{d\Omega_\Lambda}{dx} = -3\omega_\Lambda\Omega_\Lambda(1 - \Omega_\Lambda) + \Omega_\Lambda\Omega_k = -(3\omega_\Lambda - 1)\Omega_\Lambda(1 - \Omega_\Lambda). \quad (22)$$

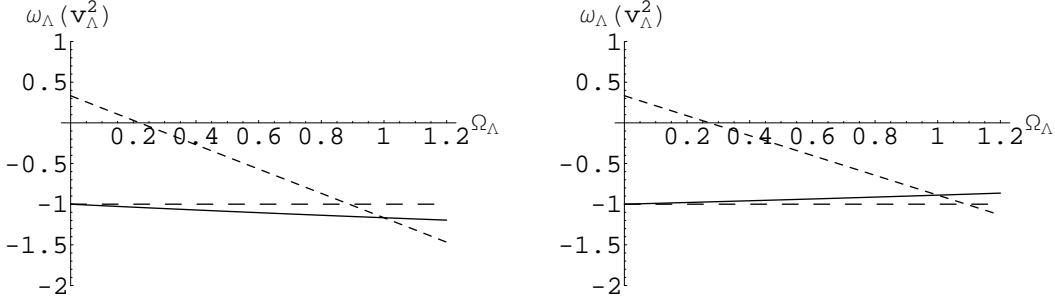


Figure 4: Two graphs for the holographic dark energy with the future event horizon for  $k \neq 0$ . The solid (dashed) lines denote the equation of state  $\omega_\Lambda$  (squared speed  $v_\Lambda^2$ ). From the left to the right, one has the graphs for  $c = 0.8$  and  $c = 1.2$ . The horizontal line denotes  $-1$ . For  $c = 1$  case, we cannot define its squared speed because of  $\omega_\Lambda = -1$ .

Finally, the squared speed takes the form

$$v_\Lambda^2 = \frac{\dot{p}_\Lambda}{\dot{\rho}_\Lambda} = \omega_\Lambda - \frac{(1 - c^2)\Omega_\Lambda(1 - \Omega_\Lambda)(c + \sqrt{\Omega_\Lambda(1 - c^2) + c^2})}{3c(c - \sqrt{\Omega_\Lambda(1 - c^2) + c^2})\sqrt{\Omega_\Lambda(1 - c^2) + c^2}}. \quad (23)$$

In the case of the nonflat universe with the future event horizon, one finds from Fig. 4 that the squared speed changes from positive value to negative one, as the universe evolves. Here one has  $v_\Lambda^2 = 0$  at  $\Omega_\Lambda = 0.22(0.27)$  for  $c = 0.8(1.2)$ . For  $c = 0.8$ , there is no discontinuity. In this sense, we insist that the nonflat effect improves the instability of the flat universe when comparing Fig.4 with Fig.1. However, the perfect fluid of holographic dark energy is still unstable for the nonflat universe. Furthermore, for  $c = 1$ , we have de Sitter spacetime of  $\omega_\Lambda = -1$ . It implies that  $\dot{\rho}_\Lambda = 0$ . Hence it is difficult to define its squared speed for de Sitter spacetime.

## 4 Discussions

We study the difference between holographic dark energy, Chaplygin gas, and tachyon model with constant potential. Especially, we calculate their squared speeds which are crucially important to determine the stability of perturbations. We find that the squared speed for holographic dark energy is always negative when imposing the future event horizon as the IR cutoff, while those for Chaplygin gas and tachyon are always non-negative. This means that the perfect fluid model for holographic dark energy is classically unstable. Hence the holographic interpretation for Chaplygin gas and tachyon is problematic. Particularly, the holographic embeddings for Chaplygin gas and tachyon [17, 21, 22] are



not guaranteed even though they have similar equations of state like the holographic dark energy.

Despite the success of holographic dark energy in obtaining an accelerating universe for  $L_\Lambda = R_{\text{FH}}$ , it may not give us a promising solution to the dark energy-dominated universe because choosing the future event horizon just means an unstable evolution. This contrasts to those for the Chaplygin gas and tachyon with constant potential.

## Acknowledgment

This work was in part supported by the Korea Research Foundation (KRF-2006-311-C00249) funded by the Korea Government (MOEHRD) and the SRC Program of the KOSEF through the Center for Quantum Spacetime (CQUeST) of Sogang University with grant number R11-2005-021.

## References

- [1] A. G. Riess *et al.*, *Astron. J.* **116** (1998) 1009 [astro-ph/9805201]; S. J. Perlmutter *et al.*, *Astrophys. J.* **517** (1999) 565 [astro-ph/9812133]; A. G. Riess *et al.*, *Astrophys. J.* **607** (2004) 665 [astro-ph/0402512]; P. Astier *et al.*, *Astron. Astrophys.* **447** (2006) 31 [arXiv:astro-ph/0510447].
- [2] M. Tegmark *et al.* [SDSS Collaboration], *Phys. Rev. D* **69** (2004) 103501 [arXiv:astro-ph/0310723];  
K. Abazajian *et al.* [SDSS Collaboration], *Astron. J.* **128** (2004) 502 [arXiv:astro-ph/0403325];  
K. Abazajian *et al.* [SDSS Collaboration], *Astron. J.* **129** (2005) 1755 [arXiv:astro-ph/0410239].
- [3] H. V. Peiris *et al.*, *Astrophys. J. Suppl.* **148** (2003) 213 [astro-ph/0302225]; C. L. Bennett *et al.*, *Astrophys. J. Suppl.* **148** (2003) 1 [astro-ph/0302207]; D. N. Spergel *et al.*, *Astrophys. J. Suppl.* **148** (2003) 175 [astro-ph/0302209].
- [4] D. N. Spergel *et al.*, arXiv:astro-ph/0603449.
- [5] U. Seljak, A. Slosar and P. McDonald, arXiv:astro-ph/0604335.
- [6] E. J. Copeland, M. Sami and S. Tsujikawa, arXiv:hep-th/0603057.

- [7] A. Upadhye, M. Ishak, and P. J. Steinhardt, Phys. Rev. D **72** (2005) 063501[arXiv:astro-ph/0411803].
- [8] A. Cohen, D. Kaplan, and A. Nelson, Phys. Rev. Lett. **82** (1999) 4971[arXiv:hep-th/9803132].
- [9] P. Horava and D. Minic, Phys. Rev. Lett. **85** (2000) 1610[arXiv:hep-th/0001145]; S. Thomas, Phys. Rev. Lett. **89** (2002) 081301.
- [10] S. D. Hsu, Phys. Lett. B **594** (2004) 13[arXiv:hep-th/0403052].
- [11] R. Horvat, Phys. Rev. D **70** (2004) 087301 [arXiv:astro-ph/0404204].
- [12] M. Li, Phys. Lett. B **603** (2004) 1[arXiv:hep-th/0403127].
- [13] Q. G. Huang and M. Li, JCAP **0408** (2004) 013 [arXiv:astro-ph/0404229].
- [14] Q-C. Huang and Y. Gong, JCAP **0408** (2004) 006[arXiv:astro-ph/0403590]; Y. Gong, Phys. Rev. D **70** (2004) 064029[arXiv:hep-th/0404030]; B. Wang, E. Abdalla and Ru-Keng Su, arXiv:hep-th/0404057; K. Enqvist and M. S. Sloth, Phys. Rev. Lett. **93** (2004) 221302 [arXiv:hep-th/0406019]; S. Nojiri and S. D. Odintsov, Gen. Rel. Grav. **38** (2006) 1285 [arXiv:hep-th/0506212]; H. Kim, H. W. Lee, and Y. S. Myung, Phys. Lett. B **628** (2005) 11[arXiv:gr-qc/0507010]; X. Zhang and F. Q. Wu, Phys. Rev. D **72** (2005) 043524[arXiv:astro-ph/0506310]; M. R. Setare, arXiv:hep-th/0609104; F. Simpson, JCAP **0703** (2007) 016 [arXiv:astro-ph/0609755]; Y. S. Myung, Phys. Lett. B **649** (2007) 247 [arXiv:gr-qc/0702032].
- [15] Y. S. Myung, Phys. Lett. B **610** (2005) 18[arXiv:hep-th/0412224]; Mod. Phys. Lett. A **27** (2005) 2035[arXiv:hep-th/0501023]; A. J. M. Medved, arXiv:hep-th/0501100.
- [16] Y. S. Myung, Phys. Lett. B **626** (2005) 1[arXiv:hep-th/0502128]. B. Wang, Y. Gong, and E. Abdalla, Phys. Lett. B **624** (2005) 141[arXiv:hep-th/0506069]; H. Kim, H. W. Lee and Y. S. Myung, Phys. Lett. B **632** (2006) 605 [arXiv:gr-qc/0509040]; M. S. Berger and H. Shojaei, Phys. Rev. D **73** (2006) 083528 [arXiv:gr-qc/0601086]; B. Hu and Y. Ling, Phys. Rev. D **73** (2006) 123510 [arXiv:hep-th/0601093]; M. S. Berger and H. Shojaei, arXiv:astro-ph/0606408; W. Zimdahl and D. Pavon, arXiv:astro-ph/0606555; M. R. Setare, Phys. Lett. B **642** (2006) 1 [arXiv:hep-th/0609069]. H. M. Sadjadi and M. Honardoost, arXiv:gr-qc/0609076; M. R. Setare, Phys. Lett. B **644** (2007) 99 [arXiv:hep-th/0610190]; K. H. Kim, H. W. Lee and Y. S. Myung, Phys. Lett. B **648** (2007) 107 [arXiv:gr-qc/0612112];

- M. R. Setare, Eur. Phys. J. C **50** (2007) 991 [arXiv:hep-th/0701085]; Q. Wu, Y. Gong, A. Wang and J. S. Alcaniz, arXiv:0705.1006 [astro-ph]; K. Y. Kim, H. W. Lee and Y. S. Myung, arXiv:0706.2444 [gr-qc].
- [17] M. R. Setare, Phys. Lett. B **648** (2007) 329 [arXiv:0704.3679 [hep-th]].
- [18] A. Sen, JHEP **0204** (2002) 048 [arXiv:hep-th/0203211].
- [19] A. Sen, JHEP **0207** (2002) 065 [arXiv:hep-th/0203265].
- [20] G. W. Gibbons, Phys. Lett. B **537** (2002) 1 [arXiv:hep-th/0204008].
- [21] M. R. Setare, arXiv:0705.3517 [hep-th].
- [22] J. Zhang, X. Zhang and H. Liu, arXiv:0706.1185 [astro-ph].
- [23] A. Y. Kamenshchik, U. Moschella and V. Pasquier, Phys. Lett. B **511** (2001) 265 [arXiv:gr-qc/0103004].
- [24] J. C. Fabris, S. V. B. Goncalves and P. E. De Souza, Gen. Rel. Grav. **34** (2002) 2111 [arXiv:astro-ph/0203441].
- [25] A. V. Frolov, L. Kofman and A. A. Starobinsky, Phys. Lett. B **545** (2002) 8 [arXiv:hep-th/0204187].
- [26] P. J. E. Peebles and B. Ratra, Rev. Mod. Phys. **75** (2003) 559 [arXiv:astro-ph/0207347].
- [27] V. Gorini, A. Kamenshchik, U. Moschella, V. Pasquier and A. Starobinsky, Phys. Rev. D **72** (2005) 103518 [arXiv:astro-ph/0504576].
- [28] H. Sandvik, M. Tegmark, M. Zaldarriaga and I. Waga, Phys. Rev. D **69** (2004) 123524 [arXiv:astro-ph/0212114].
- [29] V. Sahni, T. D. Saini, A. A. Starobinsky and U. Alam, JETP Lett. **77** (2003) 201 [Pisma Zh. Eksp. Teor. Fiz. **77** (2003) 249] [arXiv:astro-ph/0201498].
- [30] X. Zhang, Int. J. Mod. Phys. D **14** (2005) 1597 [arXiv:astro-ph/0504586].
- [31] M. R. Setare, J. Zhang and X. Zhang, JCAP **0703** (2007) 007 [arXiv:gr-qc/0611084].
- [32] H. Kim, Mon. Not. Roy. Astron. Soc. **364** (2005) 813 [arXiv:astro-ph/0408577].